Energy Storage and Saving 4 (2025) 485–499

Contents lists available at ScienceDirect

Energy Storage and Saving

journal homepage: www.keaipublishing.com/en/journals/energy-storage-and-saving/

Research article

A novel fuzzy–backward/forward sweep power flow for uncertainty management in radial distribution network with photovoltaic generation☆

Norhafidzah Mohd Saad [a,*], Muhammad Alif Mat Yusuf [a], Mohammad Fadhil Abas [a], Dwi Pebrianti [b], Norazila Jaalam [a], Suliana Ab. Ghani [a]

[a] Faculty of Electrical & Electronics Engineering Technology, Universiti Malaysia Pahang Al-Sultan Abdullah, Pekan, Pahang, 26600, Malaysia
[b] Kuliyyah of Engineering, International Islamic University Malaysia, Kuala Lumpur, 50728, Malaysia

ARTICLE INFO

Keywords:
Photovoltaic distributed generation (PVDG)
Backward/forward sweep power flow
Fuzzy logic
Radial distribution network
Grey Wolf Optimizer (GWO)

ABSTRACT

This research presented a novel framework of fuzzy-backward/forward sweep (F-BFS) power flow to address uncertainties in radial distribution networks with photovoltaic generation. The F-BFS framework integrated fuzzified values to model uncertainty parameters in radial distribution network power flow analysis, whereas the Grey Wolf Optimizer (GWO) was employed to optimize photovoltaic distributed generation (PVDG) placement and sizing, aiming to minimize power losses and improve voltage deviations. Load uncertainties in the residential, commercial, and industrial sectors were modeled using triangular fuzzy membership functions derived from real-world data representing Malaysian urban loads. Simulations on the 33-bus distribution network validated the approach and demonstrated its effectiveness in handling fuzzy uncertainties across three load sectors. The findings showed that the proposed F-BFS-GWO method significantly reduced the total power losses and improved the voltage profiles. Under high load conditions, active power losses were reduced by approximately 28.04% in residential, 46.06% in commercial, and 46.24% in industrial sectors at the highest membership degree in the fuzzy set, compared to the scenario without photovoltaic generation. The critical voltage magnitudes at the weakest bus under high-load conditions in the fuzzy set also improve significantly, reaching nearly 1.0 p.u. The main contributions of this work are the integration of fuzzy-logic within a BFS framework to manage multi-sector load uncertainties, coupled with a hybrid F-BFS–GWO algorithm that enhances system planning and optimization under the risk of uncertainty of photovoltaic generation and load demand.

1. Introduction

Electricity providers are focusing on how to address rising environmental concerns and energy needs. Considering sustainability and increasing energy demands, solar power plants, especially photovoltaic distributed generation (PVDG) plants, have been of immense significance. Unlike traditional centralized power systems, PVDG decentralizes power generation and disperses it over numerous areas rather than just one centralized system. By improving the voltage profiles and optimizing the utilization of system equipment, small generators are connected to distribution systems to meet load demands while profitably benefiting from reduced power losses [1,2]. The location of PVDGs has a substantial influence on voltage profiles, power losses, and system reliability; hence, it is an important component that needs to be considered in power system planning [3,4]. It is easier to site smaller generators, they have lower capital costs and are closer to heavy loads which reduces transmission costs [5,6]. The installation of PVDG in the network provides a few advantages, including a reduction in power loss and reduced energy undelivered cost. This also results in other benefits, such as lower peak load operating costs, improved voltage profiles, and higher load factors [7,8].

Despite these advantages, PVDG can cause negative impacts such as increases in power losses and frequency and voltage deviations. According to the study by Saad et al. [9], when the size of the PVDG is increased beyond the statutory limits, it results in higher losses. Thus, the PVDG size must be capped and optimized to efficiently manage the network within a distribution substation area. Additionally, it is necessary to minimize losses by placing PVDGs in appropriate areas in the distribution network [10]. Because the problem is nonlinear, it is challenging to solve it using conventional mathematical methods [11]. The

☆ Peer review under responsibility of Xi'an Jiaotong University

* Corresponding author.
E-mail address: norhafidzah@umpsa.edu.my (N.M. Saad).

https://doi.org/10.1016/j.enss.2025.05.002
Received 28 January 2025; Received in revised form 24 April 2025; Accepted 12 May 2025
Available online 6 August 2025

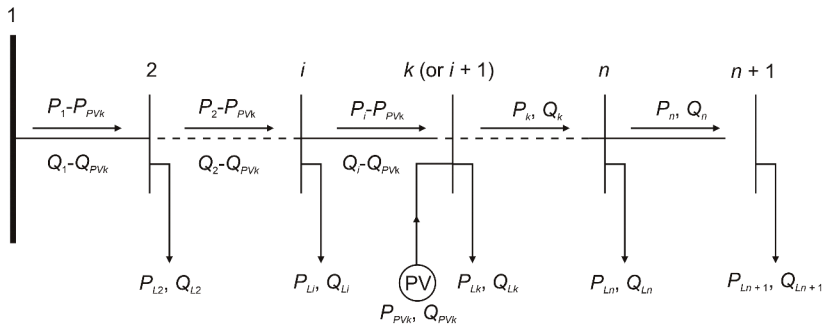

Fig. 1. The radial system with photovoltaic distributed generation (PVDG).

Table 1
Fuzzy-logic rules for fuzzy–backward/forward sweep (F-BFS).

Rule No.	Condition (inputs)			Output (response)	
Rule 1	if $\Delta F_{P_L,\,fuzzy}$	and$\Delta F_{Q_L,\,fuzzy}$	is L then	$\Delta \boldsymbol{X}_{P_{Loss},\,fuzzy}$	is L
Rule 2	if $\Delta F_{P_L,\,fuzzy}$	and$\Delta F_{Q_L,\,fuzzy}$	is M then	$\Delta \boldsymbol{X}_{P_{Loss},\,fuzzy}$	is M
Rule 3	if $\Delta F_{P_L,\,fuzzy}$	and$\Delta F_{Q_L,\,fuzzy}$	is H then	$\Delta \boldsymbol{X}_{P_{Loss},\,fuzzy}$	is H
Rule 4	if $\Delta F_{P_L,\,fuzzy}$	and$\Delta F_{Q_L,\,fuzzy}$	is L then	$\Delta \boldsymbol{X}_{Q_{Loss},\,fuzzy}$	is L
Rule 5	if $\Delta F_{P_L,\,fuzzy}$	and$\Delta F_{Q_L,\,fuzzy}$	is M then	$\Delta \boldsymbol{X}_{Q_{Loss},\,fuzzy}$	is M
Rule 6	if $\Delta F_{P_L,\,fuzzy}$	and$\Delta F_{Q_L,\,fuzzy}$	is H then	$\Delta \boldsymbol{X}_{Q_{Loss},\,fuzzy}$	is H
Rule 7	if $\Delta F_{P_L,\,fuzzy}$	and$\Delta F_{Q_L,\,fuzzy}$	is L then	$\Delta \boldsymbol{X}_{V_{pu},\,fuzzy}$	is H
Rule 8	if $\Delta F_{P_L,\,fuzzy}$	and$\Delta F_{Q_L,\,fuzzy}$	is M then	$\Delta \boldsymbol{X}_{V_{pu},\,fuzzy}$	is M
Rule 9	if $\Delta F_{P_L,\,fuzzy}$	and$\Delta F_{Q_L,\,fuzzy}$	is H then	$\Delta \boldsymbol{X}_{V_{pu},\,fuzzy}$	is L

Note: ΔF is the power parameters in fuzzy number and $\Delta \boldsymbol{X}$ is the state vector.

placement of PVDG in distribution systems is a multi-objective optimization problem. As per previous studies [12–14], the metaheuristics optimization-based method can help determine the optimal location and size of PVDG.

One promising approach is the use of machine learning models such as neural networks [15,16] and Gaussian-based methods [17,18]. Neural networks have been applied to forecast the solar power output and optimize the scheduling of photovoltaic (PV) systems in hybrid energy setups, significantly improving the performance of smart grids. In addition, Gaussian- and probability-based methods have been widely used to deal with uncertainties in renewable energy generation [19], particularly for solar irradiance prediction, which employs a probabilistic approach for modeling the uncertainty in solar radiation and its impact on PV generation.

Optimization algorithms for determining the lowest or highest objective functions have been widely explored in the application of electrical power systems by many researchers. For instance, the optimization method based on electric eel foraging [20] aims to determine

Algorithm 1
Fuzzy-backward/forward sweep (F-BFS) incorporated Grey Wolf Optimizer (GWO) pseudo-code.

```
START
    Load profile data
    Generate fuzzy load model
    Set k = number of generated fuzzy data
    FOR each number of generated fuzzy data
      Load radial distribution data
      IF F-BFS power flow not converge
        Calculate P_L = P_Lold × fuzzy data in p.u.
        Calculate Q_L = Q_Lold × fuzzy data in p.u.
        Run F-BFS power flow for each membership values
      END IF
    END FOR
    Compute bus voltage and power losses in fuzzy membership
    RETURN bus voltage and power losses
  END
```

the locations of distributed generation (DG) units in distribution networks while accounting for several technical conditions, such as circuit reconfigurations and power factor limits. Kadir et al. [21] developed an improved gravitational search algorithm to determine the appropriate placement and sizing for DG units considering load growth. A study by Fu et al. [22] presented a method using a genetic algorithm (GA) to determine the appropriate allocation and size of DG in a distribution network, considering voltage and harmonic limitations, with the objective of minimizing network losses. Jaalam et al. [23] explored the metaheuristic approach, emphasizing the role of the Grey Wolf Optimizer (GWO) in enhancing low-voltage ride-through in grid-connected PV systems.

Previous studies have examined numerous methods for evaluating renewable generation integration in power systems. According to the study by Chibani et al. [24], the inclination angle (β) of the PV system, along with the presence of fins, also affects the efficiency of solar power generation. However, owing to the risk of uncertain behavior, such as the geographical spread and complexity of power systems, including load demand and renewable generation, accurate system identification remains a challenge. Power system operators rarely have access to exact specifications for loads or generation during power flow studies. Thus, evaluating uncertainty-related input parameters, such as the load and renewable generation, is crucial. There are two main sources of uncertainty parameters: (1) randomness, which pertains to the variability characteristic, and (2) incompleteness of parameter values, owing to the full factors affecting the system being unknown. Uncertainty due to randomness can be mitigated through statistical analysis. These uncertain parameters are often represented by probabilistic descriptions such as the probability density function (PDF) [25].

Saad et al. [26] developed a Monte Carlo-embedded hybrid variant mean-variance mapping optimization for PVDG allocation in a distribution network considering uncertainties in solar irradiance and load demand. Some studies [27,28] demonstrated the allocation of DG based on the reliability performance in the distribution network. A Monte Carlo simulation methodology was employed to evaluate system reliability performance. Yin et al. [29] suggested a chance-constrained operation model based on probabilistic power balance that accounts for PV and load uncertainty. Li et al. [30] developed a principal component analysis and high-dimensional model for probabilistic power flow and highlighted its advantages over the traditional point-estimate method approach.

Previous research has effectively employed probability power flow analysis to enhance the power flow calculations that incorporate uncertainties. However, inadequate statistical data can result in biased estimates and inaccurate models [31]. Thus, making assumptions based on human expertise might provide insight into parameter values that represent cognitive uncertainties, as opposed to statistical uncertainties. Fuzzy logic offers a way to model uncertainty by allowing for degrees of truth rather than classical true or false. Several literature reviews have successfully utilized fuzzy-logic to improve power-flow calculations, reflecting its growing applications in power systems.

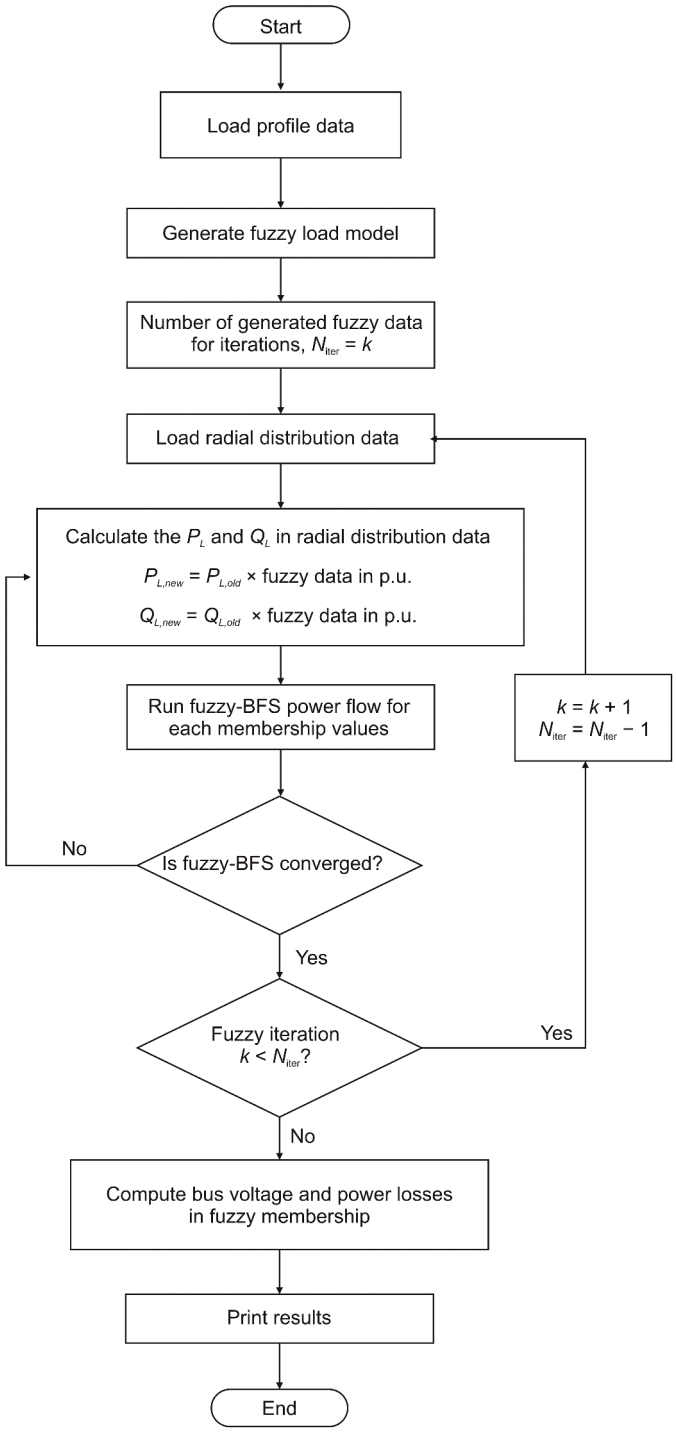

Fig. 2. Flowchart for fuzzy-backward/forward sweep (F-BFS) power flow.

Wu et al. [32] demonstrated the effectiveness of random fuzzy theory in addressing wind turbines, PV generation, and the load uncertainty of distribution networks. A study by Zaki et al. [33] discussed a fuzzy approach for fault identification in an active distribution network with both grid-connected and off-grid PV systems. In another study, Sedaghat et al. [34] explored fuzzy load uncertainty for optimal DG allocation based on Biogeography-based Optimization (BBO). The work in Samala and Kotapuri [35] further adopted fuzzy methodologies by presenting a hybrid approach that combines a fuzzy logic controller for the fitness function. In addition, Alkayyali and Tutunji [36] adopted Particle Swarm Optimization (PSO), and Maher et al. [37] implemented Ant-lion Optimization (ALO) for optimal DG planning.

However, while these studies have laid the groundwork for optimization applications in power systems, they often do not integrate fuzzy logic with advanced load flow analysis to create a hybrid algorithm capable of effectively managing uncertainties in load flow with renewable energy integration. This gap has inspired the development of new methods: fuzzy-backward/forward sweep (F-BFS) power flow, which effectively applies fuzzy logic to represent power system uncertainties in radial distribution networks. By incorporating fuzzy parameters, these approaches enhance power flow analysis by accounting for uncertainties, enabling improved decision-making in the management of DG systems.

This presents a significant gap that the current research aims to address by developing a novel framework that combines the F-BFS power flow with GWO, thereby providing a more comprehensive solution for PVDG allocation considering uncertainty. The contributions of this study are as follows.

(1) A possibility approach based on human expertise was employed in this study to effectively manage the risks of uncertainty in PV generation and load demands.
(2) This study leveraged the strengths of fuzzy logic and the BFS power flow method to develop a hybrid F-BFS algorithm. By utilizing fuzzified values within the F-BFS framework, this approach accommodates a wider range of uncertainty parameters in power flows and losses within distribution networks.
(3) Furthermore, the integration of GWO enhanced the optimization process, enabling the identification of optimal PVDG locations that maximize system performance while minimizing losses. This combination not only addresses a gap in the existing literature, but also contributes significantly to ongoing efforts toward sustainable energy management. The hybrid approach considers fuzzy uncertainties and simultaneously optimizes the placement and sizing of PV systems in distribution networks.

Research focused on radial distribution systems has highlighted the benefits of the hybrid F-BFS method that incorporates GWO in identifying critical components affected by both PV generation and load uncertainties. This leads to improved decision-making for network operators. This study examined three types of fuzzified load uncertainty models, including residential, commercial and industrial load.

The remainder of this paper is organized as follows. Section 2 addresses the problem formulation of F-BFS and GWO, covering the mathematical models, membership functions, objective function, and constraints, as well as the flowchart of the proposed algorithm. Section 3 details the findings obtained using 33-bus radial distribution systems and discusses the results. Section 4 provides a summary of the findings.

2. Problem formulation

2.1. BFS power flow

The BFS power flow method was developed by Shirmohammadi et al. [38], which utilizes fundamental Kirchhoff's laws to solve radial or weakly meshed power system structures. The problem formulation for the radial distribution network with PVDG was derived based on Fig. 1.

The BFS power flow was used to analyze the convergence of the iterative process. In Fig. 1, a branch is connected between buses i and k (or $i + 1$). The effective active and reactive powers flowing through the link from bus i to bus k (or $i + 1$) can be calculated in the backward direction from the last bus, as given by:

$$P_i = P_{i+1} + P_{L_k} + P_{loss,\ i} \tag{1}$$

$$Q_i = Q_{i+1} + Q_{L_k} + Q_{loss,\ i} \tag{2}$$

where P_i and Q_i represent the active and reactive power flowing out of

Algorithm 2
F-BFS incorporated GWO pseudo-code.

```
START
  Initialize fuzzy data
  Generate GWO population
  Set k = 1 (iteration counter)
  Set N_iter = 100 (maximum number of iterations)
  WHILE k ≤ N_iter DO
    Check for convergence criteria satisfaction
    IF convergence criteria are satisfied THEN
      Display results (voltage profiles, power losses)
      STOP
    ELSE
      Run fuzzy backward/forward sweep (F-BFS) power flow
      Update positions and wolves based on the optimization technique
      Calculate distance to prey
      Update positions and ensure diversity for optimal location and size of PVDG
      k = k + 1 (increment iteration counter)
    END IF
  END WHILE
  Generate results in fuzzy membership bus voltage and power losses.
  RETURN bus voltage and power losses
END
```

the bus, respectively. P_{i+1} and Q_{i+1} are the active and reactive powers at bus k (or $i+1$), R_i and X_i denote the line resistance and reactance connecting bus i and bus k (or $i+1$), P_{L_k} and Q_{L_k} represent the active and reactive load powers at bus k (or $i+1$), respectively.

The power loss in the line between buses i and k (or $i+1$) is calculated as follows:

$$P_{loss\ (i,\ i+1)} = \frac{(P_i)^2 + (Q_i)^2}{|V_i|^2} R_i \tag{3}$$

$$Q_{loss\ (i,\ i+1)} = \frac{(P_i)^2 + (Q_i)^2}{|V_i|^2} X_i \tag{4}$$

The total apparent power loss $S_{T,\ loss\ (i,\ i+1)}$ can be written as:

$$S_{T,\ loss\ (i,\ i+1)} = \sum_{bus=1}^{N_{buses}} P_{loss\ (i,\ i+1)} + j \sum_{bus=1}^{N_{buses}} Q_{loss\ (i,\ i+1)} \tag{5}$$

The magnitude and angle of the voltage at each bus are computed in the forward direction. The current flowing through the branch with the branch impedance linked between buses i and k (or $i+1$) is calculated as:

$$I_i = \frac{(V_i \angle \delta_i) - (V_{i+1} \angle \delta_{i+1})}{Z_{(i,\ i+1)}} \tag{6}$$

The PVDG unit on bus k acts as a negative load. As a result, the active and reactive powers associated with PVDG penetration can be calculated as:

$$P_i = P_{i+1} + P_{L_k} + P_{loss,\ i} - P_{PV} \tag{7}$$

$$Q_i = Q_{i+1} + Q_{L_k} + Q_{loss,\ i} - Q_{PV} \tag{8}$$

The active and reactive power losses in the line between buses i and k (or $i+1$) associated with PVDG penetration can be calculated as:

$$P_{loss\ (i,\ i+1),\ PV} = \frac{\left(P_i - P_{PV,\ k}\right)^2 + \left(Q_i - Q_{PV,\ k}\right)^2}{|V_i|^2} R_i \tag{9}$$

$$Q_{loss\ (i,\ i+1),\ PV} = \frac{\left(P_i - P_{PV,\ k}\right)^2 + \left(Q_i - Q_{PV,\ k}\right)^2}{|V_i|^2} X_i \tag{10}$$

A deterministic power flow analysis was used to evaluate the operation of the power system. It calculates the power flow and system states based on the specified power generation and load demand within a given network configuration. This analysis involves solving the equations to determine the power balance of the system. The equations below define the network power balance that the power flow distribution must satisfy:

$$\sum_{bus=1}^{N_{buses}} P_{generation} - \left[\sum_{bus=1}^{N_{buses}} P_{load} + P_{loss}\right] = 0 \tag{11}$$

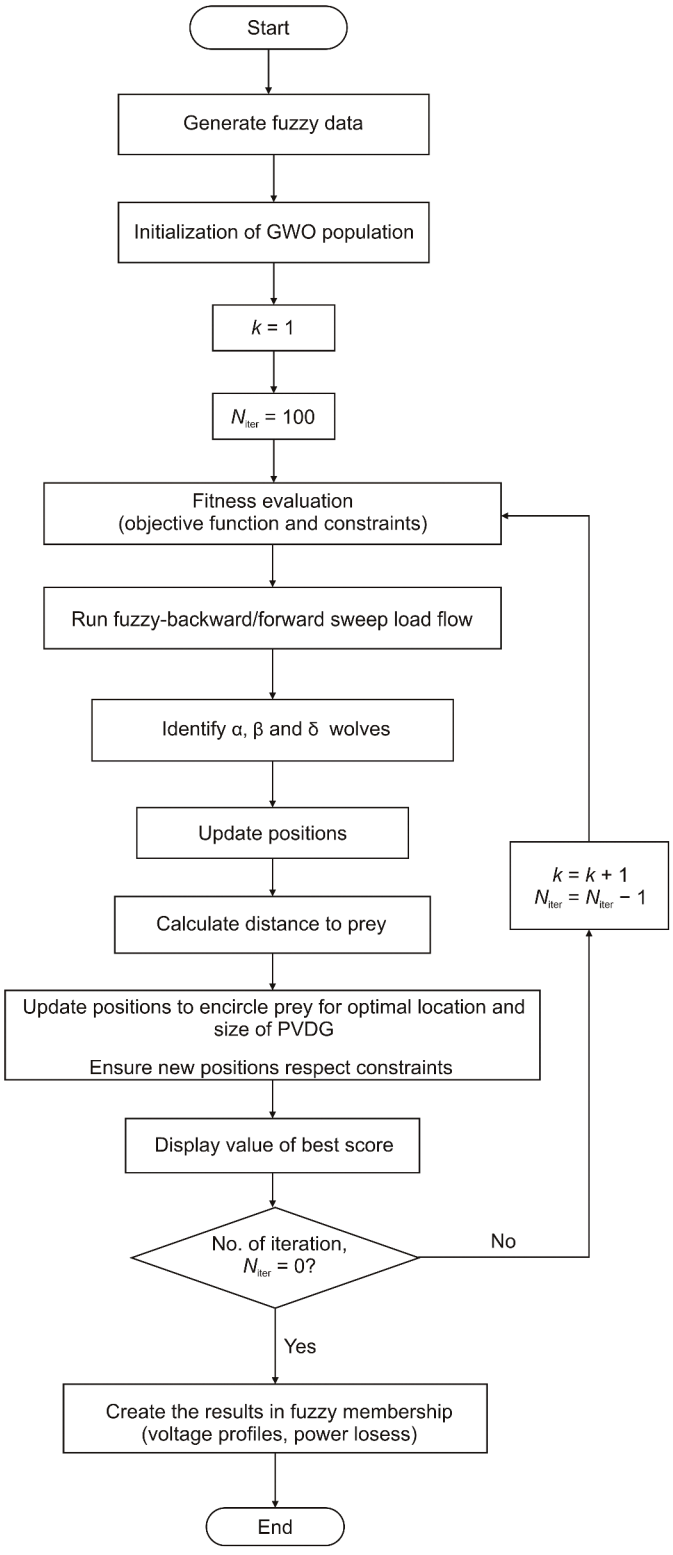

Fig. 3. Searching process for photovoltaic distributed generation (PVDG) allocation in the radial distribution network using fuzzy – backward/forward sweep (F-BFS) incorporated Grey Wolf Optimizer (GWO).

$$\sum_{bus=1}^{N_{buses}} Q_{generation} - \left[\sum_{bus=1}^{N_{buses}} Q_{load} + Q_{loss}\right] = 0 \tag{12}$$

2.2. F-BFS power flow

Modern power networks with renewable energy sources, in this case with PVDG penetrations and fluctuating load demands, require further consideration because deterministic load flow analysis fails to account for power system uncertainties. The power flow equations are nonlinear owing to the power-voltage relationship. Analytical solutions for power flow analysis are difficult to obtain; therefore, numerical methods are recommended. Eq. (13) represents a set of nonlinear algebraic equations in a steady state, where g denotes the set of nonlinear algebraic equations representing the power balance of the network, x is the state vector comprising state variables x_i, and u is a vector comprising the input variables. The power flow problem involves determining the solution (zero) of a set of nonlinear equations, known as power-balance equations, based on an initial guess (x_0).

$$g(x,u) = 0 \tag{13}$$

The fuzzy power flow analysis begins with the nonlinear algebraic Eq. (13) and incorporates power system uncertainty into the input vector (u). The input vector (u) is divided into two components that contain deterministic variables and another containing uncertain variables, labeled as ΔX which can be defined using a membership function. The adjustment of ΔX at each node of the system is proportional to ΔF.

$$\Delta X = fuz\ (\Delta F) \tag{14}$$

fuz denotes the fuzzy logic function. The fuzzy power flow method is based on the BFS equation, and the update of the system state is repeatedly performed via fuzzy logic control, rather than using deterministic load flow approaches. The fuzzy power flow equations can be derived based on the corrected state of the vector comprising the state and input variables at each bus in the system.

In this study, loads were categorized into three types: residential, commercial, and industrial. These loads are represented as fuzzy numbers. The dataset encompassed urban load data, with the assumption that only weekday daily loads were considered, excluding weekends. The collected data included a range from low to maximum load occurrences, which were used to design the fuzzy-logic membership functions. These functions are essential for analyzing the load demand uncertainty and its impact on the power distribution network.

To fuzzify these loads, a fuzzy-logic approach was employed, with the load values represented by triangular membership functions. The triangular membership function of a fuzzy set is defined using three parameters: *P*min, *P*hp, and *P*max. *P*min represents the lowest value in the dataset. *P*max is the maximum value in the dataset and *P*hp is the highest possibility of occurrence. The membership function $\mu(x)$ of a triangular fuzzy number is determined as follows:

$$\mu(x) = \begin{cases} 0 & \\ \dfrac{x - Pmin}{Php - Pmin} & If\ x\ < Pmin \\ \dfrac{Pmax - x}{Pmax - Php} & IfPmin \le x \le Php \\ 0 & If\ Php < x \le Pmax \\ & If\ x > Pmax \end{cases} \tag{15}$$

Membership functions for each type of load were employed to determine the degree of membership for any given load within the defined range. This fuzzification method aids in the management of uncertainty and fluctuation in load estimates, enabling a more robust analysis and optimization in the context of DG and load management. The load data were fuzzified into a corresponding fuzzy signal $\Delta F_{P_L,\ fuzzy}$ and $\Delta F_{Q_L,\ fuzzy}$, using three linguistic variables: low (L), medium (M), and high (H). In fuzzy logic, rules are applied to perform analysis. In this analysis, nine fuzzy rules were developed. The rules are conditional statements that use fuzzy logic to support decision making. The complete rule base is outlined as follows (Table 1).

Running the F-BFS algorithm on the distribution network yields fuzzy values for the power flow through branches and substations. Consequently, active and reactive power losses are expressed as fuzzy numbers. The pseudocode for the F-BFS power flow is presented in Algorithm 1, and the corresponding flowchart is shown in Fig. 2.

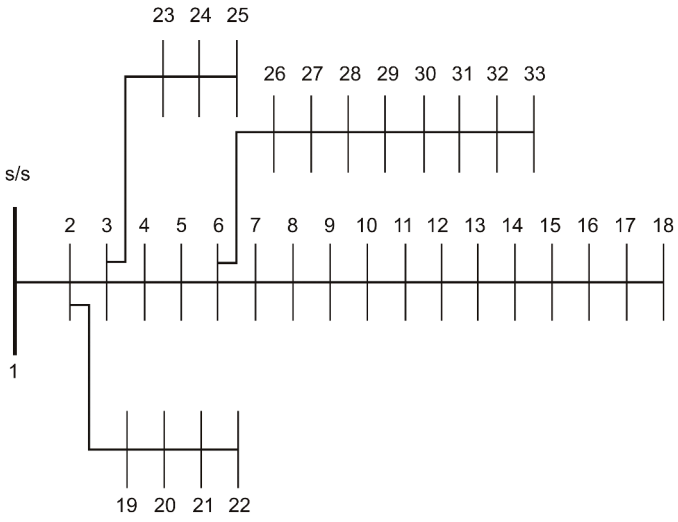

Fig. 4. 33-bus radial configuration.

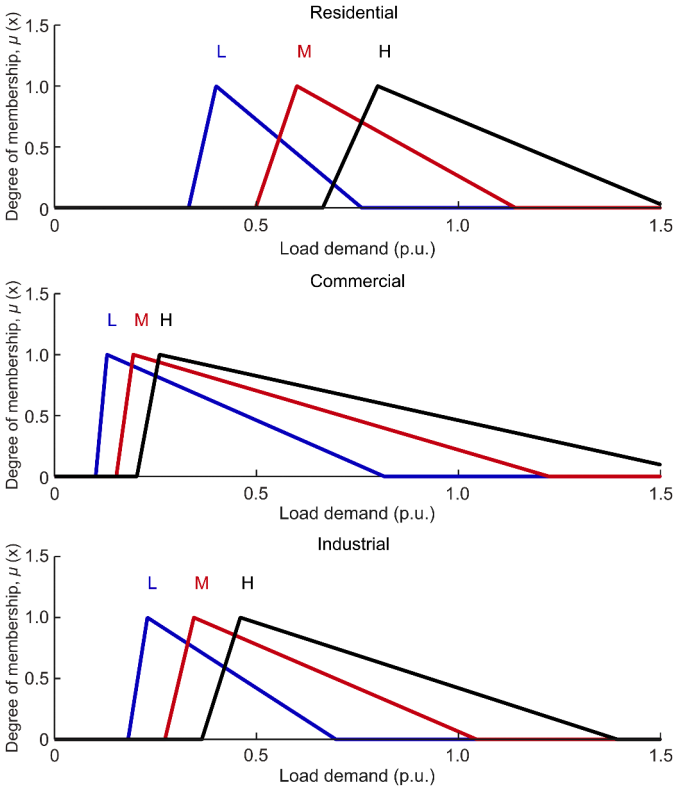

Fig. 5. Fuzzy membership function for residential, commercial and industrial loads demands.

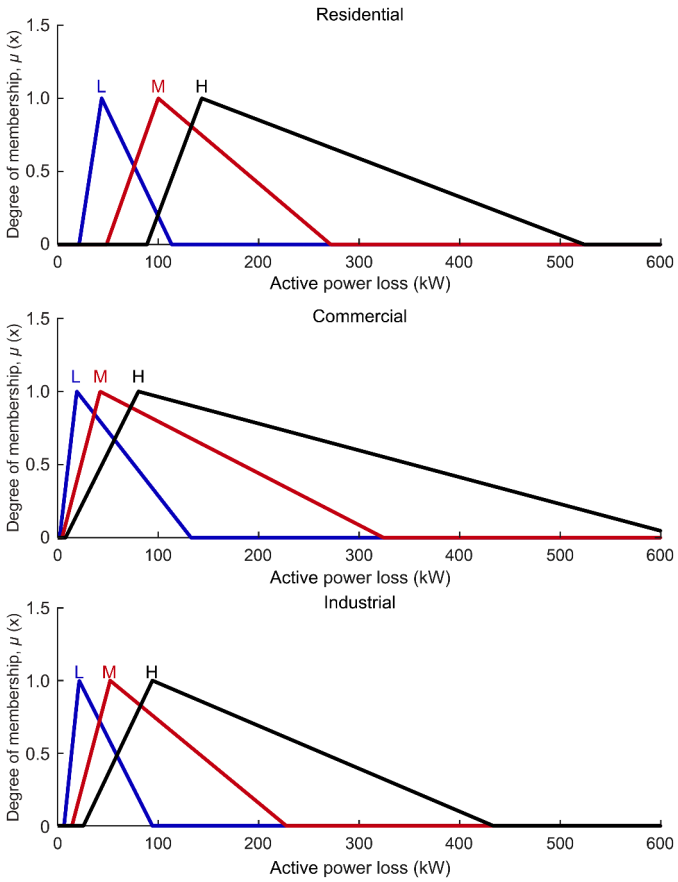

Fig. 6. Fuzzy membership function for active power losses in residential, commercial and industrial loads.

2.3. Objective function and constraints

Instead of using a crisp value, the variables were specified as fuzzy variables. For instance, the active power P_i at bus i can be expressed using a fuzzy set $\widetilde{P}_i$, with a membership function μP_i, where μ denotes the degree of membership of P_i in the fuzzy set.

2.3.1. Objective function

Under equality and inequality constraints, objective functions were formulated to minimize the total losses of active and reactive power as well as the voltage deviations at all buses:

$$\begin{aligned} &\text{Minimize } F = [f_1, f_2, f_3] \\ &f_1 = \sum_{N_{\text{bus no}=1}^{\text{buses}}} \widetilde{P}_{T,\text{loss}} \\ &f_2 = \sum_{\text{bus no}=1}^{N_{\text{buses}}} \widetilde{Q}_{T,\text{ loss}} \\ &f_3 = \sum_{\text{bus no}=1}^{N_{\text{buses}}} \left|\widetilde{V}_i - \widetilde{V}_{ref}\right| \end{aligned} \tag{16}$$

where $\widetilde{P}_{T,\text{ loss}}$, $\widetilde{Q}_{T,\text{ loss}}$, $\widetilde{V}_i$, and $\widetilde{V}_{ref}$ represent the fuzzy variables corresponding to the total active and reactive power losses, voltage at bus i, and the reference nominal voltage, respectively.

2.3.2. Network power balance

The optimization must satisfy the active and reactive power balance equations, incorporating fuzzy-logic, as follows:

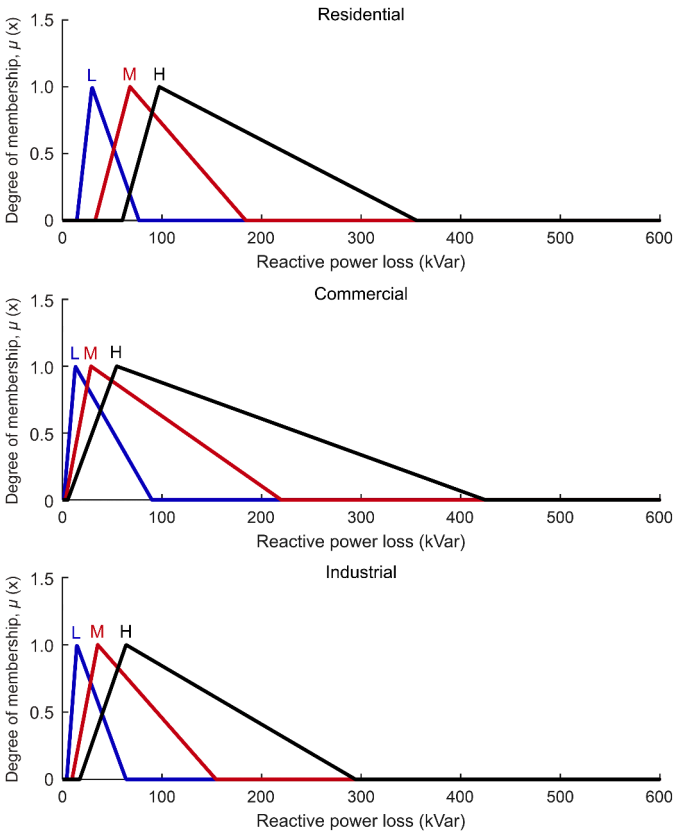

Fig. 7. Fuzzy membership function for reactive power losses in residential, commercial and industrial loads.

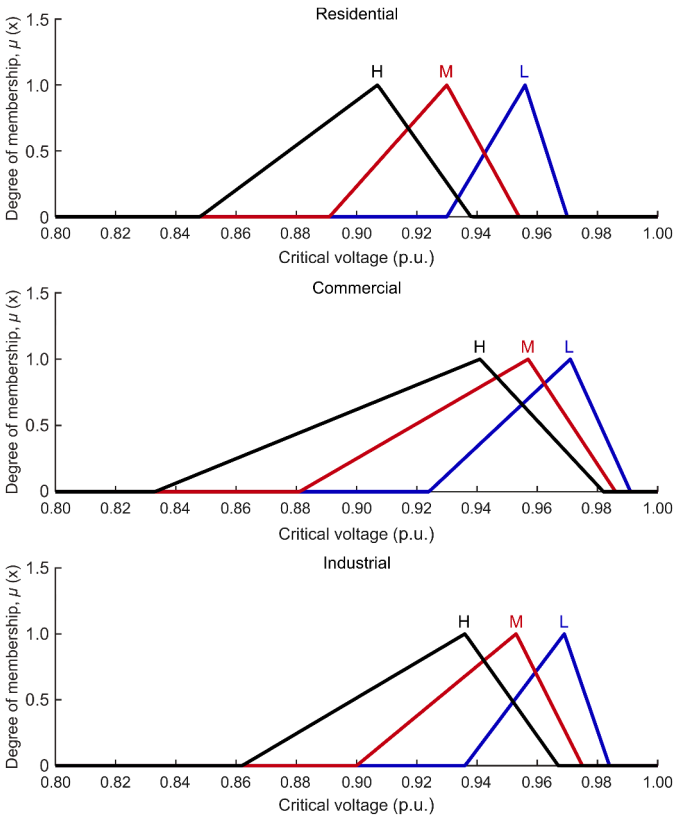

Fig. 8. Fuzzy membership function for critical voltage in residential, commercial and industrial loads at bus 18.

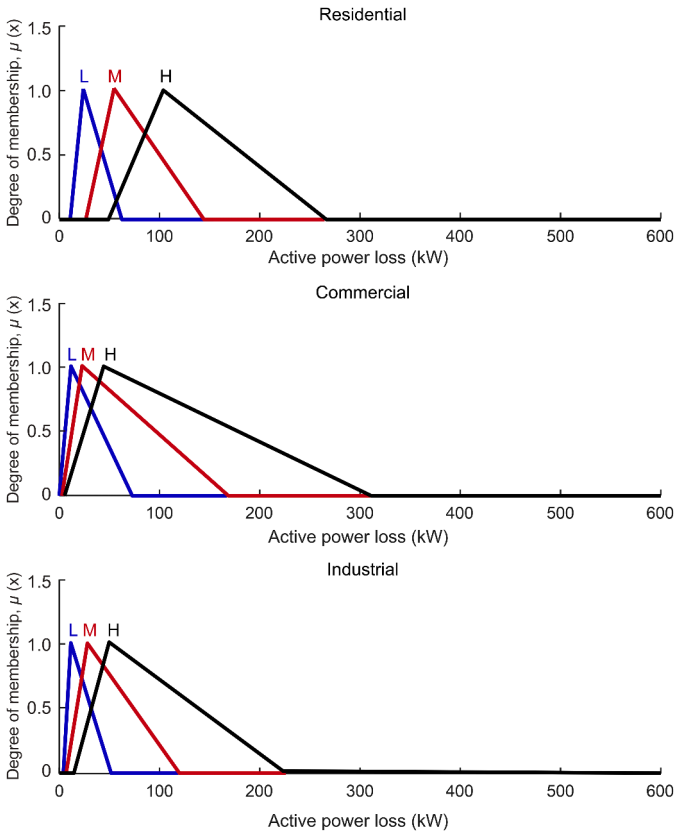

Fig. 9. Fuzzy membership function of active power losses in residential, commercial and industrial loads in 33-bus radial distribution network (RDN) with photovoltaic distributed generation (PVDG) integration at bus 6.

$$\widetilde{P}_i + \widetilde{P}_{pv,\ i+1} = \widetilde{P}_{i+1} + \widetilde{P}_{L_k} + \frac{(\widetilde{P}_i)^2 + (\widetilde{Q}_i)^2}{|\widetilde{V}_i|^2} R_i \tag{17}$$

$$\widetilde{Q}_i + \widetilde{Q}_{pv,\ i+1} = \widetilde{Q}_{i+1} + \widetilde{Q}_{L_k} + \frac{(\widetilde{P}_i)^2 + (\widetilde{Q}_i)^2}{|\widetilde{V}_i|^2} X_i \tag{18}$$

where $\widetilde{P}_i$, $\widetilde{Q}_i$, and $\widetilde{V}_i$ denote the fuzzy variables representing the active power, reactive power, and voltage, respectively, at bus *i*.

2.3.3. Bus voltage boundaries

The voltage boundaries must be maintained within safe operating limits. Eq. (19) ensures that the voltage magnitude at each bus remains within an acceptable range.

$$\widetilde{V}_{min} \le |\widetilde{V}_i| \le \widetilde{V}_{max}\ i = 1,\ 2, \ldots,\ n\ bus \tag{19}$$

2.3.4. PVDG operating capacity

The PVDG capacity limit is governed by the inequality constraints given below. $\widetilde{P}^{min}_{PVDG}$ capacity was set to zero, and the $\widetilde{P}^{max}_{PVDG}$ capacity was determined based on the total active load demand. The value of $\widetilde{P}^{max}_{PVDG}$ varied for each client, depending on the total active power load.

$$\widetilde{P}^{min}_{PVDG} \le \widetilde{P}_{PVDG} \le \widetilde{P}^{max}_{PVDG} \tag{20}$$

The maximum penetration of PVDG in the distribution system must satisfy the following condition:

$$\sum_{i=1}^{n} \widetilde{P}_{PVDG,\ i} \le \sum_{i=1}^{n} \widetilde{P}_{Load,\ i}, i = 1,\ 2, \cdots,\ n\ \text{bus} \tag{21}$$

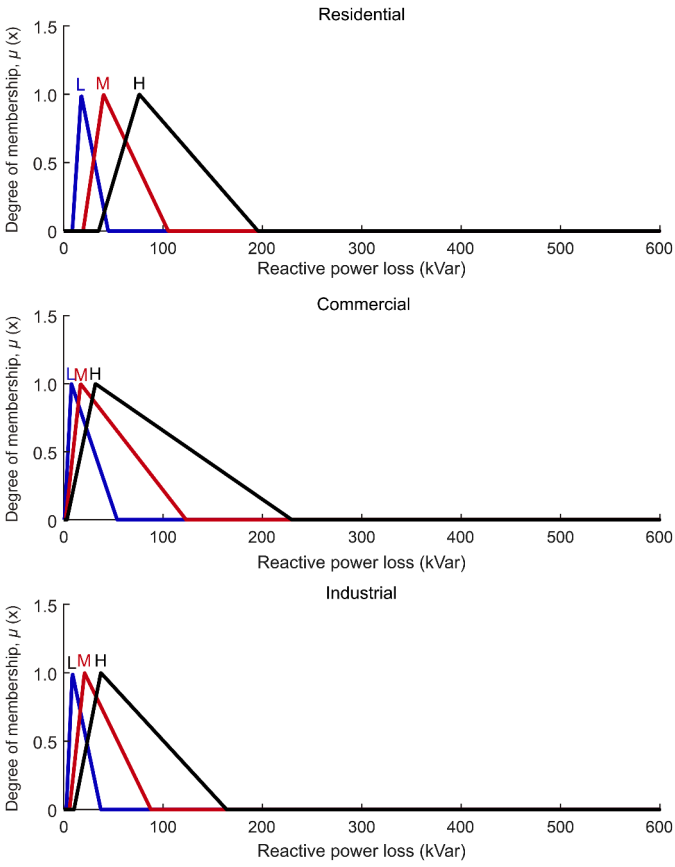

Fig. 10. Fuzzy membership function of reactive power losses in residential, commercial and industrial loads in 33-bus radial distribution network (RDN) with photovoltaic distributed generation (PVDG) integration at bus 6.

2.3.5. PVDG location

Except for the slack bus, the PVDG site can be connected to any bus in the network.

$$2 \le PVDG_{site} \le \max\ No.\ of\ buses \tag{22}$$

2.4. F-BFS incorporated GWO

GWO was proposed by Mirjalili et al. [39]. The algorithm is based on the social hierarchy of grey wolves. In a wolf pack, members respond to a dominant social order with search agents adjusting their positions based on the best performance. Alpha (α) is the leader of the gry wolves. It determines all decisions. All the other pack members must obey these commands. Beta (β) is the second-highest rank, assisting Alpha in decision making and enforcing its commands. Delta (δ) provides a feedback channel for wolf reporting. Finally, omega (ω) is the follower and has the lowest ranking in the hierarchy.

In this study, the GWO was initialized with 10 numbers of search agents and a maximum iteration of 100. The pseudocode for the search process used for PVDG allocation in the radial distribution network is provided in Algorithm 2. A flowchart representing the optimization process for PVDG placement is shown in Fig. 3.

2.5. Test case: 33-bus radial distribution network (RDN)

Fig. 4 illustrates the topology of a standard 33-bus RDN. The peak load demands for this test case were 3,715 and 2,300 kVar. The system data for the 33-bus radial configuration are provided by Baran and Wu

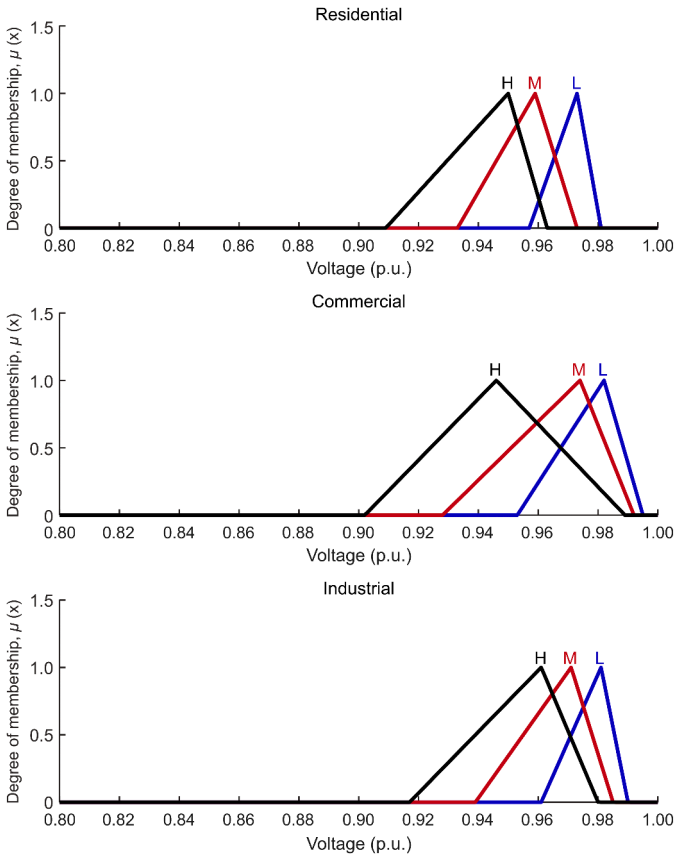

Fig. 11. Fuzzy membership function of critical voltage in residential, commercial and industrial loads in 33-bus radial distribution network (RDN) with photovoltaic distributed generation (PVDG) integration at bus 6.

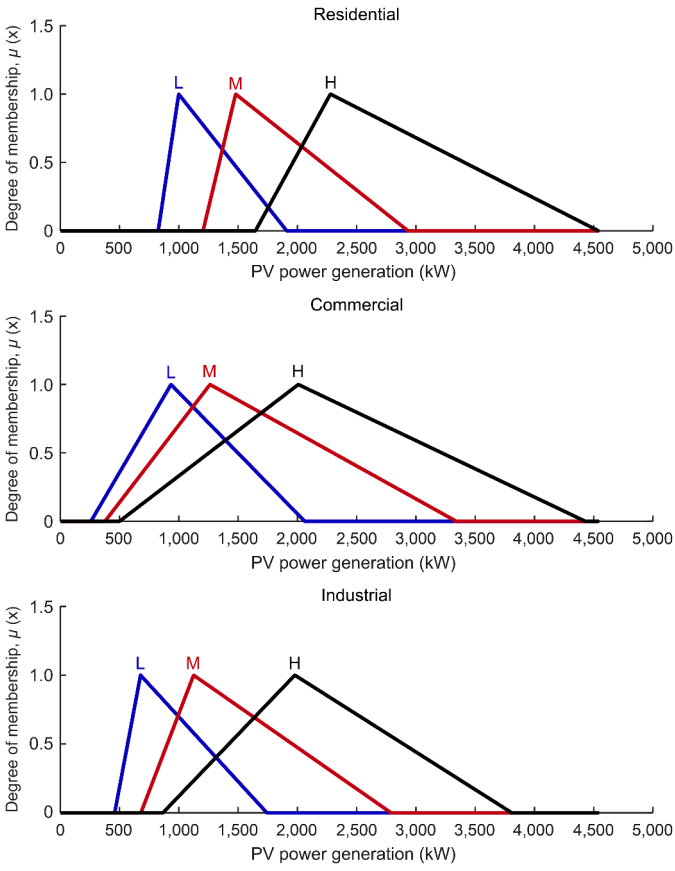

Fig. 12. Fuzzy membership function of PV power generation in residential, commercial and industrial loads in 33 bus radial distribution network (RDN) with photovoltaic distributed generation (PVDG) at bus 6.

[40]. The network was selected because of its high relevance to real-world distribution systems with radial configurations. Load profiles were modeled using one-year data from Tenaga Nasional Berhad (TNB) and recorded at 15-minute intervals for urban residential, commercial, and industrial consumers. The data were segmented by sector minimum (L_{min}), highest possibility (L_{hp}), and maximum (L_{max}) values, and were extracted to construct triangular fuzzy membership functions representing low, medium, and high load conditions. For each load type, the PVDG capacity was capped based on the total active power load of the bus, according to the constraints described in Section 2.3. The PV generation uncertainty is represented using triangular membership functions, which are discussed in Section 3.

3. Results and discussion

3.1. Fuzzy load membership functions

Fig. 5 shows the fuzzy membership functions for residential, commercial, and industrial load demands categorized as low (L), medium (M), and high (H). These functions were derived from the urban load profile data collected in Malaysia. Triangular membership functions were used, defined by three key values: minimum (*P*min), highest possibility (*P*hp), and maximum (*P*max) load levels. These fuzzy memberships were generated by capturing the range from the minimum to maximum load occurrences. Random data points from the dataset were then used to calculate new fuzzy load data for each bus in the 33-bus radial network. These fuzzified load values were applied to each bus in the 33-bus radial network, where the F-BFS power flow algorithm was used to compute the branch flows, voltage profiles, and total power losses.

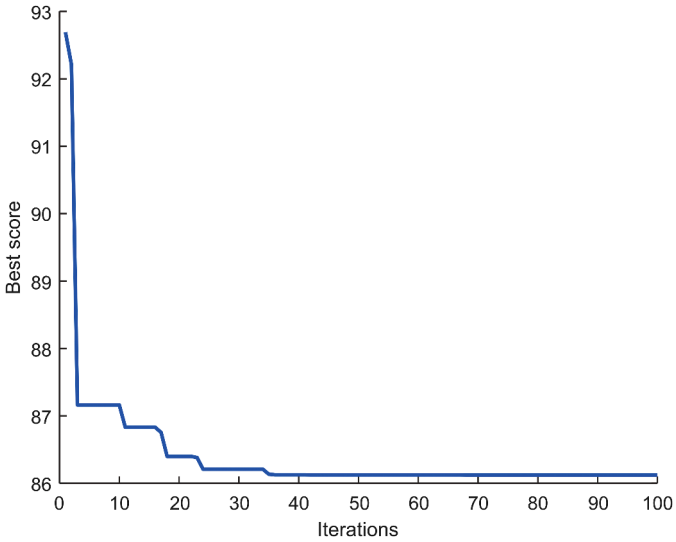

Fig. 13. Convergence rate for the case in residential at high (H) load conditions.

3.2. F-BFS for the case without PVDG

Three cases were examined: residential, commercial, and industrial load profiles for the case without the PVDG allocation. The backward and forward propagation iterative equations performed the distribution of the power flow. The power in each branch was calculated using

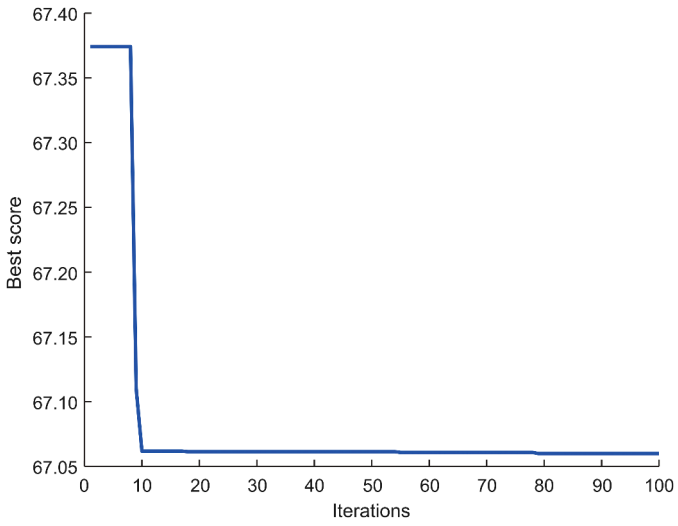

Fig. 14. Convergence rate for the case in commercial at high (H) load conditions.

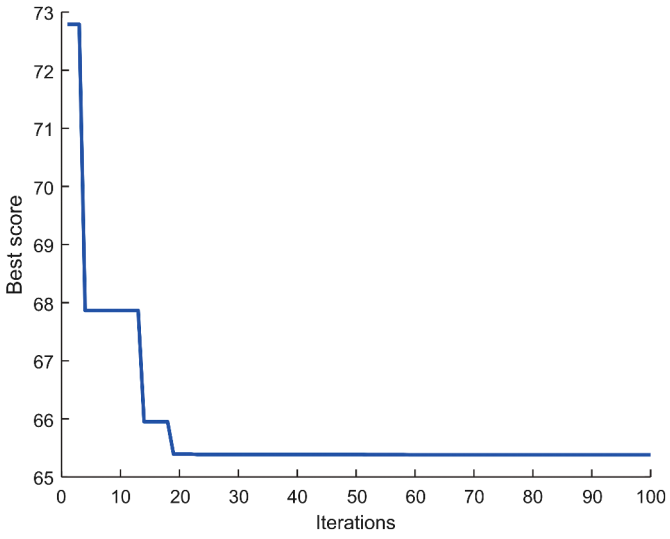

Fig. 15. Convergence rate for the case in industrial at high (H) load conditions.

Table 2
Optimal photovoltaic distributed generation (PVDG) location and size.

Load uncertainty	PVDG location (Bus No.)	PVDG size (MW)
Residential	6	2.2786
Commercial	6	2.0078
Industrial	6	1.9787

backward propagation. Forward propagation is then used to determine the voltage magnitude at each bus.

The fuzzy membership functions for the power loss and voltage profiles were derived based on the applied fuzzy rules. Among the load types, the residential scenarios exhibited the highest total power losses and critical bus voltage magnitudes compared to the other load categories. These membership functions capture the uncertainty in system losses and voltage behavior under each load category.

Referring to Figs. 6 and 7, the analysis of total power losses across different load sectors reveals distinct patterns and magnitudes, as shown by the fuzzy membership functions. Among the sectors, residential loads exhibited the highest power losses, with active power losses ranging from approximately 20 kW to 530 kW and the corresponding reactive power losses ranging from 15 kVar to 356 kVar, corresponding to higher degrees of membership and greater uncertainty. The highest membership values for active power losses in residential loads were 43.8 kW (L), 100.1 kW (M), and 143.4 kW (H). Whereas the highest membership values for reactive power losses were 29.6 kVar (L), 67.8 kVar (M), and 97.1 kVar (H). This variability reflects the diverse consumption patterns in residential areas and the absence of PVDG support.

In comparison, commercial loads experienced active power losses between 2 kW and 600 kW with corresponding reactive power losses between 1.4 kVar and 425 kVar. The highest membership values occurred at 19.1 kW (L), 42.3 kW (M), and 80.4 kW (H), reflecting increased losses during peak business hours. Whereas the highest membership values for reactive power losses were 12.9 kVar (L), 28.6 kVar (M), and 54.5 kVar (H). Effective peak demand management in this sector could help reduce losses and improve network stability.

Industrial loads showed active power losses ranging from 6.4 kW to 430 kW and reactive power losses ranging from 4.3 kVar to 295 kVar. Despite the narrower loss range, significant power losses were observed during periods of high industrial activity. The highest membership values for industrial loads were 21.4 kW (L), 52.3 kW (M), and 94.3 kW (H). Whereas the highest membership values for reactive power losses were 14.5 kVar (L), 35.4 kVar (M), and 63.9 kVar (H). These findings emphasize the distinct contribution of each load sector to overall system performance and highlight the importance of implementing sector-specific strategies for minimizing losses and enhancing network reliability.

Fig. 8 presents the fuzzy representation of the critical voltage magnitudes at bus 18, identified as the weakest bus across all load types. The voltage range varied by sector, with residential loads showing the highest variability owing to diverse consumption behaviors. The critical voltage range for residential loads ranged from 0.85 to 0.97 p.u., with the highest membership values at 0.96 p.u. (L), 0.93 p.u. (M), and 0.91 p.u. (H). Commercial loads had a wider range between 0.83 to 0.99 p.u., with peak membership values at 0.97 p.u. (L), 0.96 p.u. (M), and 0.94 p.u. (H), respectively. Industrial loads showed a slightly narrower range of 0.86 to 0.98 pu, with corresponding peak values at 0.97 p.u. (L), 0.95 p.u. (M), and 0.94 p.u. (H). These voltage uncertainties reflect the characteristic consumption patterns and the operating conditions of each sector. In the absence of PVDG integration, voltage magnitudes under high load conditions fell below the International Electrotechnical Commision (IEC)-recommended threshold of 0.95 p.u., indicating potential reliability concerns. The membership function analysis confirmed that voltage violations were more likely to occur during peak load periods, particularly in residential and commercial sectors.

3.3. Results of F-BFS incorporated GWO for the case with PVDG

Three load cases (residential, commercial, and industrial) were examined using PVDG allocation. The proposed F-BFS method, integrated with the GWO, was used to perform the power flow distribution using backward and forward sweep iterations. The GWO assisted in optimizing the placement and sizing of PVDG units within the radial distribution network. When combined with fuzzy logic, GWO effectively addressed uncertainties in both load profiles and PV generation, enabling robust decision making under uncertain operating conditions. Figs. 9–11 illustrate the resulting fuzzy membership functions for the total system losses and critical bus voltages with PVDG integration at bus 6.

Referring to Figs. 9 and 10, the power loss graphs illustrate the variations and uncertainty across the residential, commercial, and industrial load sectors, represented by fuzzy membership levels: low (L), medium (M), and high (H). A higher membership degree indicates a greater likelihood of power loss, reflecting fluctuating consumption patterns. The integration of PVDG significantly reduced power losses across all sectors, improved voltage profiles, and enhanced system

Table 3
Comparison of active power loss in 33–bus radial distribution network.

Load case	Pmin (kW)		Php (kW)		Pmax (kW)	
	F-BFS (without PV)	F-BFS (with PV)	F-BFS (without PV)	F-BFS (with PV)	F-BFS (without PV)	F-BFS (with PV)
Residential load						
Low	21.429	11.741	43.803	23.926	113.498	60.782
Medium	48.696	26.514	100.107	54.709	271.666	144.042
High	88.877	47.777	143.360	103.165	523.979	266.098
Commercial load						
Low	2.049	1.141	19.097	10.482	132.721	72.074
Medium	4.533	2.522	42.269	22.989	324.123	167.352
High	7.928	4.401	80.404	43.371	625.275	310.726
Industrial load						
Low	6.408	3.531	21.430	11.741	94.334	50.718
Medium	14.259	7.886	52.277	28.391	227.562	119.308
High	25.693	14.044	94.334	50.718	433.532	224.405

Note: PV: photovoltaic; F-BFS: fuzzy-backward/forward sweep.

Table 4
Comparison of reactive power loss in 33–bus radial distribution network.

Load case	Qmin (kVar)		Qhp (kVar)		Qmax (kVar)	
	F-BFS (without PV)	F-BFS (with PV)	F-BFS (without PV)	F-BFS (with PV)	F-BFS (without PV)	F-BFS (with PV)
Residential load						
Low	14.495	8.632	29.638	17.581	76.881	44.709
Medium	32.963	19.495	67.791	39.943	184.201	105.203
High	60.185	35.147	97.117	75.908	355.785	195.551
Commercial load						
Low	1.384	0.838	12.918	7.706	89.904	53.769
Medium	3.064	1.852	28.607	16.910	219.859	123.146
High	5.360	3.232	54.435	31.889	424.773	229.613
Industrial load						
Low	4.333	2.598	14.495	8.633	63.883	37.302
Medium	9.640	5.791	35.384	20.876	154.257	87.774
High	17.381	10.328	63.883	37.302	294.249	163.973

Note: PV: photovoltaic; F-BFS: fuzzy-backward/forward sweep.

Table 5
Comparison of critical voltage in 33–bus radial distribution network.

Load case	Vmin (p.u.)		Vhp (p.u.)		Vmax (p.u.)	
	F-BFS (without PV)	F-BFS (with PV)	F-BFS (without PV)	F-BFS (with PV)	F-BFS (without PV)	F-BFS (with PV)
Residential load						
Low	0.930	0.957	0.956	0.973	0.970	0.981
Medium	0.891	0.933	0.930	0.952	0.954	0.973
High	0.848	0.909	0.907	0.950	0.938	0.963
Commercial load						
Low	0.924	0.953	0.971	0.982	0.991	0.995
Medium	0.881	0.928	0.957	0.974	0.986	0.992
High	0.833	0.902	0.941	0.964	0.982	0.989
Industrial load						
Low	0.936	0.961	0.969	0.981	0.984	0.990
Medium	0.900	0.939	0.953	0.971	0.975	0.985
High	0.862	0.917	0.936	0.961	0.967	0.980

Note: PV: photovoltaic; F-BFS: fuzzy-backward/forward sweep.

reliability compared with the base case without PVDG.

In the residential sector, the active and reactive power losses without PVDG were 20−530 kW and 15−356 kVar (Figs. 6 and 7). After integrating PVDG at bus 6, losses were reduced to 11.7−266.1 kW and 8.6−196.0 kVar (Figs. 9 and 10). The highest membership values under L, M, and H loads were 23.9 kW + j17.6 kVar, 54.7 kW + j39.9 kVar, and 103.2 kW + j75.9 kVar, indicating a 20%−50% reduction in losses at the highest membership degree in the fuzzy set.

Table 6
Results of F-BFS-GWO and F-BFS-GA for residential load uncertainty in 33-bus radial distribution network.

Output (response)	Parameter	PV configuration	Load case		
			Low	Medium	High
Active power loss	Pmin (kW)	F-BFS-GWO	11.741	26.514	47.777
		F-BFS-GA	11.471	26.514	47.777
	Php (kW)	F-BFS-GWO	23.926	54.709	103.165
		F-BFS-GA	23.926	55.578	103.165
	Pmax (kW)	F-BFS-GWO	60.782	144.042	266.098
		F-BFS-GA	60.782	144.595	268.309
Reactive power loss	**Qmin (kVar)**	F-BFS-GWO	8.632	19.495	35.147
		F-BFS-GA	8.633	19.495	35.147
	Qhp (kVar)	F-BFS-GWO	17.581	39.943	75.908
		F-BFS-GA	17.581	40.876	75.910
	Qmax (kVar)	F-BFS-GWO	44.709	105.203	195.551
		F-BFS-GA	44.709	105.203	196.04
Voltage	**Vmin (p.u.)**	F-BFS-GWO	0.957	0.933	0.909
		F-BFS-GA	0.957	0.933	0.909
	Vhp (p.u.)	F-BFS-GWO	0.973	0.959	0.950
		F-BFS-GA	0.973	0.959	0.945
	Vmax (p.u.)	F-BFS-GWO	0.981	0.973	0.963
		F-BFS-GA	0.981	0.973	0.963

Note: PV: photovoltaic; F-BFS-GWO: fuzzy-backward/forward sweep-Grey Wolf Optimizer; F-BFS-GA: fuzzy-backward/forward sweep-genetic algorithm.

For the commercial sector, losses without PVDG dropped from 2−600 kW and 1.4−425 kVar (Figs. 6 and 7) to 1.2−310.7 kW and 0.8−229.6 kVar (with PVDG, Figs. 9 and 10). Peak membership values at L, M, and H were 10.5 kW + j7.7 kVar, 23 kW + j16.9 kVar, and 43.4 kW + j31.9 kVar, reflecting about 40%−46% loss reduction at the highest membership degree in the fuzzy set.

The industrial sector experienced the most consistent improvement. Without PVDG, losses ranged from 6.4−433.5 kW and 4.3−294.2 kVar (Figs. 6 and 7). With PVDG losses were reduced to 3.5−224.4 kW and 2.6−164 kVar (Figs. 9 and 10). Maximum membership values under L, M, and H loads were 11.7 kW + j8.6 kVar, 28.4 kW + j20.9 kVar, and 50.7 kW + j37.3 kVar showing about 40%−46% reductions at the highest membership degree in the fuzzy set.

This analysis highlights the value of sector-based uncertainty modeling and demonstrates that PVDG integration is highly effective in reducing power losses and improving the reliability of distribution systems under uncertain load conditions.

Fig. 11 illustrates the fuzzified critical voltage magnitudes after PVDG installation at bus 6 with bus 18, which was identified as the weakest node in the network. To highlight the improvement achieved through PVDG integration, comparative voltage ranges from the case without PVDG (Fig. 8) are also referenced. The voltage range for residential loads improved from 0.85 to 0.97 p.u. (without PVDG) to 0.91 to

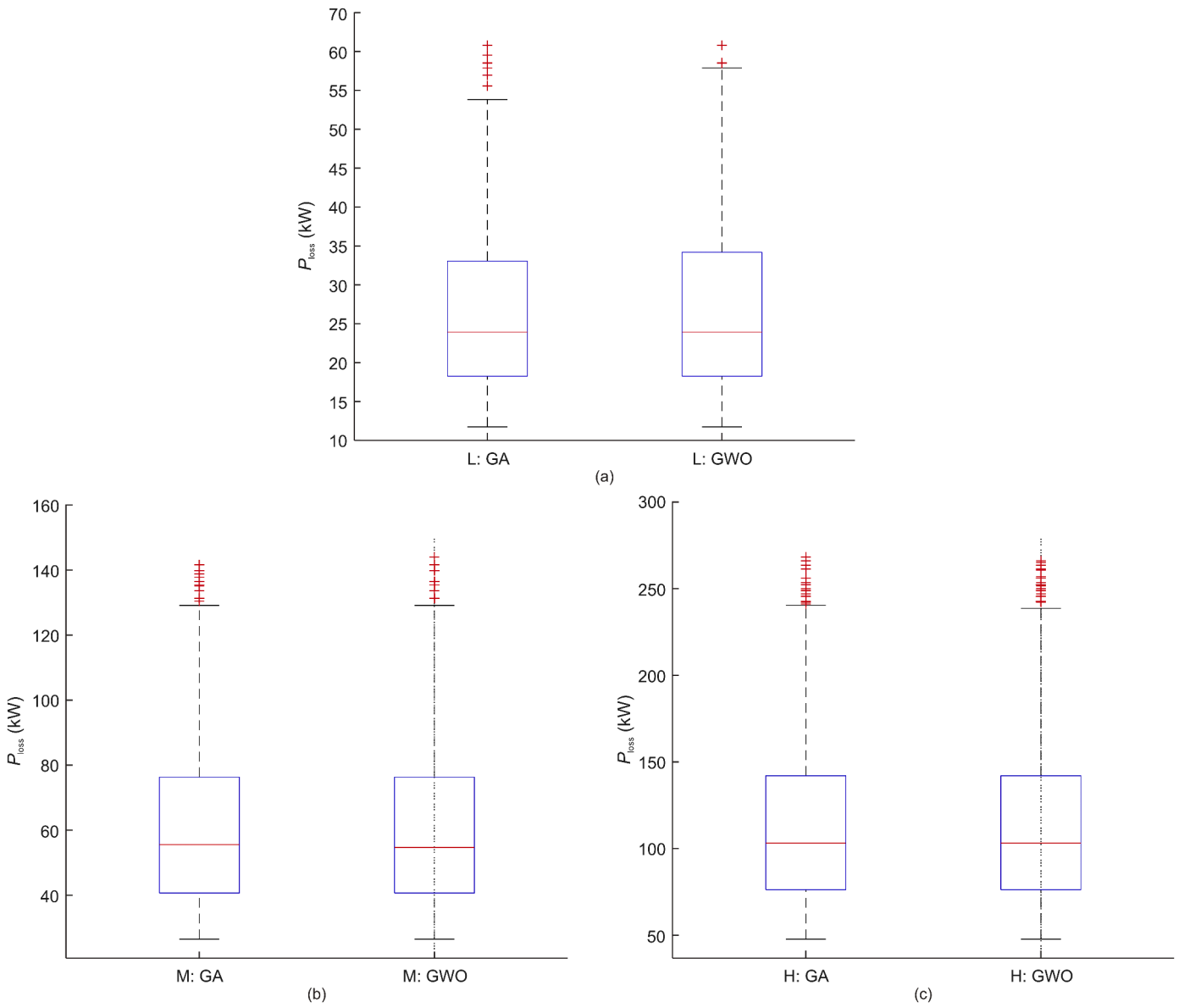

Fig. 16. Boxplots of fuzzy backward/forward sweep-Grey Wolf Optimizer (F-BFS-GWO) and fuzzy backward/forward sweep-genetic algorithm (F-BFS-GA) for active power loss (P_{loss}) considering fuzzy load uncertainty. (a) Low, (b) medium, (c) high.

0.98 p.u. (with PVDG). For commercial loads, the range improved at 0.90 to 1.0 p.u. (with PVDG) from 0.83 to 0.99 p.u. (without PVDG). Industrial loads, while less sensitive to voltage drops, showed an improved range from 0.86 to 0.98 p.u. (without PVDG) to 0.92 to 0.99 p.u. (with PVDG).

In terms of highest membership values, residential loads showed improvements from 0.96 p.u., 0.93 p.u., and 0.90 p.u. (without PVDG) to 0.97 p.u., 0.95 p.u., 0.95 p.u. (with PVDG). For commercial loads, critical voltage levels increased slightly from 0.97 p.u., 0.96 p.u., and 0.94 p.u. to 0.98 p.u., 0.97 p.u., and 0.96 p.u. Industrial loads also experienced improvements, with values rising from 0.97 p.u., 0.95 p.u., and 0.93 p.u. to 0.98 p.u., 0.97 p.u., and 0.96 p.u.

Overall, the membership function analysis confirmed that PVDG integration leads to better voltage regulation across all load sectors. These improvements help maintain the voltage within the IEC-recommended limits, thereby enhancing the reliability and safety of the distribution system under varying load conditions.

Fig. 12 shows the fuzzified value for PV power generation in residential, commercial, and industrial loads with PVDG installed at bus 6. The output membership functions reflect the uncertainty of the PV output across the radial distribution system. Based on these fuzzy values, the optimization algorithm identifies the optimal size and placement of PVDG units.

Figs. 13–15 show the convergence rates of the fuzzy GWO algorithm under high (H) load conditions for each load sector. The F-BFS method, integrated with GWO, effectively optimized PVDG allocation in the presence of fuzzy uncertainties. The final optimal PVDG locations and sizes are presented in Table 2.

3.4. Comparative analysis

Case studies with and without PV generation were analyzed to compare the performance of active and reactive power loss reduction, voltage profile improvement, and load uncertainty handling. The loads were considered triangular fuzzy numbers. The results indicate that F-BFS incorporating GWO is an efficient way to allocate PVDG to decrease losses and improve critical voltage magnitudes while considering uncertainty. When handling load uncertainty, the GWO algorithm

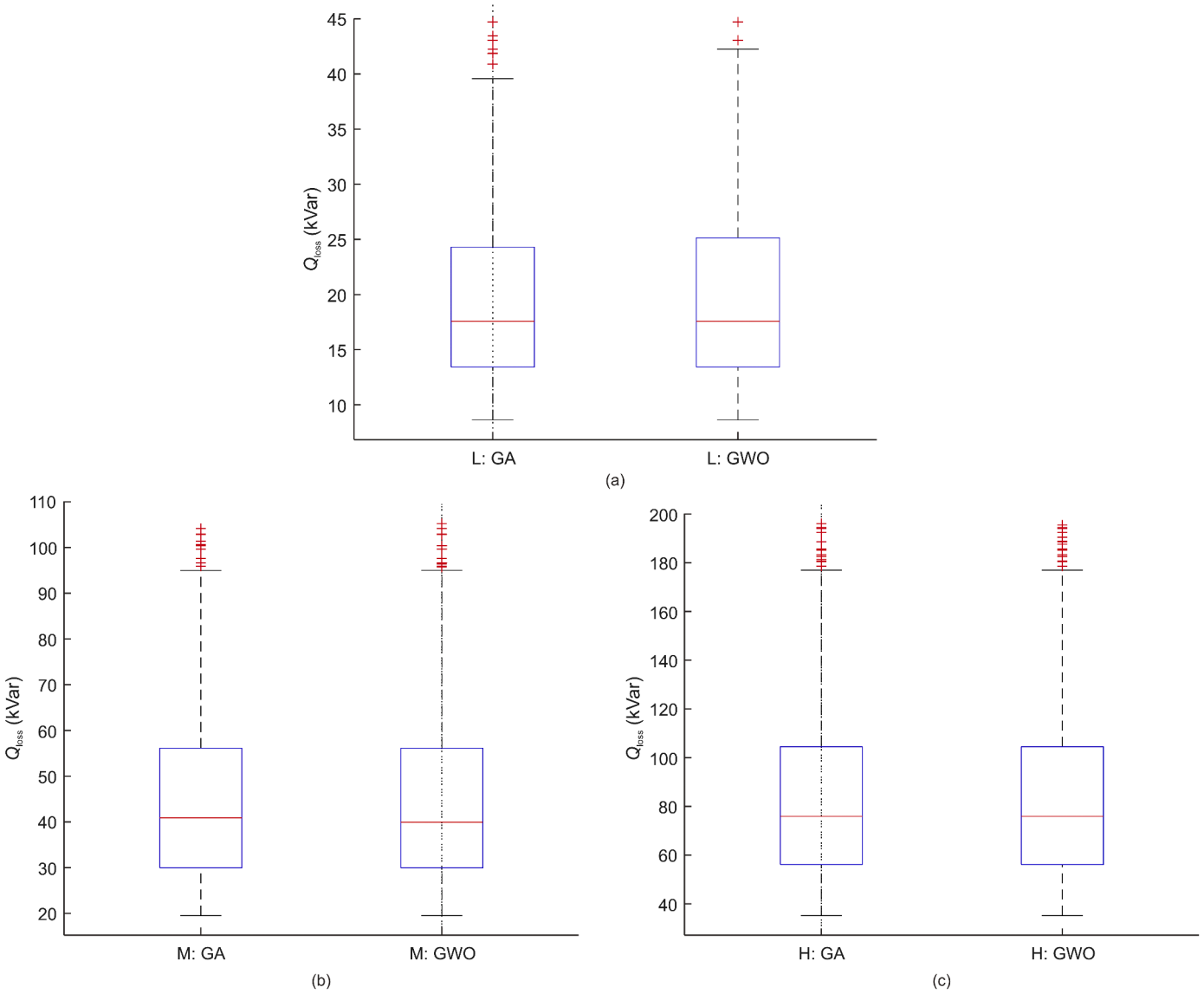

Fig. 17. Boxplots of fuzzy backward/forward sweep-Grey Wolf Optimizer (F-BFS-GWO) and fuzzy backward/forward sweep-genetic algorithm (F-BFS-GA) for reactive power loss (Q_{loss}) considering fuzzy load uncertainty (a) Low, (b) Medium, (c) High.

combined with fuzzy logic effectively optimized the PV location and improved performance. Fuzzy membership functions allow for adaptive responses to varying loads under fuzzy uncertainty.

Owing to the fuzzy load flow considerations in the F-BFS, the active and reactive power losses and critical voltages at the critical bus were assumed to be three distinct values, as determined by the triangular fuzzy membership function described in Section 2. These values represent the lower and upper limits, indicated by the minimum and maximum indices, and the highest membership value, indicated by the highest probability (hp).

Tables 3 and 4 present a comprehensive comparison between the load configurations with (F-BFS-GWO) and without (F-BFS) PVDG systems. The active and reactive power losses in all load sectors decreased by adding PVDG to the network. The integration of photovoltaic systems has resulted in substantial improvements across multiple performance metrics. Moreover, the implementation of PVDG effectively reduced the active and reactive power losses, as shown in Tables 2 and 3, thereby enhancing energy efficiency. These results underscore the significant benefits of PVDG, not only in improving energy reliability, but also in promoting sustainable energy practices. Furthermore, the PVDG effectively minimized active power losses and reactive power losses, demonstrating its role in enhancing operational efficiency and reducing energy wastage.

Table 5 presents a comparison of the performance for the critical voltage with (F-BFS-GWO) and without PVDG systems (F-BFS).

The incorporation of PVDG systems yielded substantial improvements in voltage regulation within the distribution networks. Specifically, the integration of PVDG enhances voltage stability, which is crucial for maintaining consistent power quality in commercial establishments. These findings highlight the suitability of PVDG, where reliability, cost-effectiveness, and environmental sustainability are critical considerations. In terms of voltage profile improvement, the case with PVDG shows improved voltage profiles with fewer deviations from the desired range, thereby enhancing the stability and reliability of the network. Without PVDG, voltage profile fluctuations and deviations lead to reduced stability, particularly during peak demand periods. The voltage profiles in Table 5 show a notable enhancement, ensuring a more stable and reliable power supply to the distribution areas.

For further benchmarking of the proposed formulation, the results were compared with those obtained using the fuzzy backward/forward sweep-genetic algorithm (F-BFS-GA) method to validate the findings of the proposed F-BFS-GWO approach. Table 6 presents the results of F-

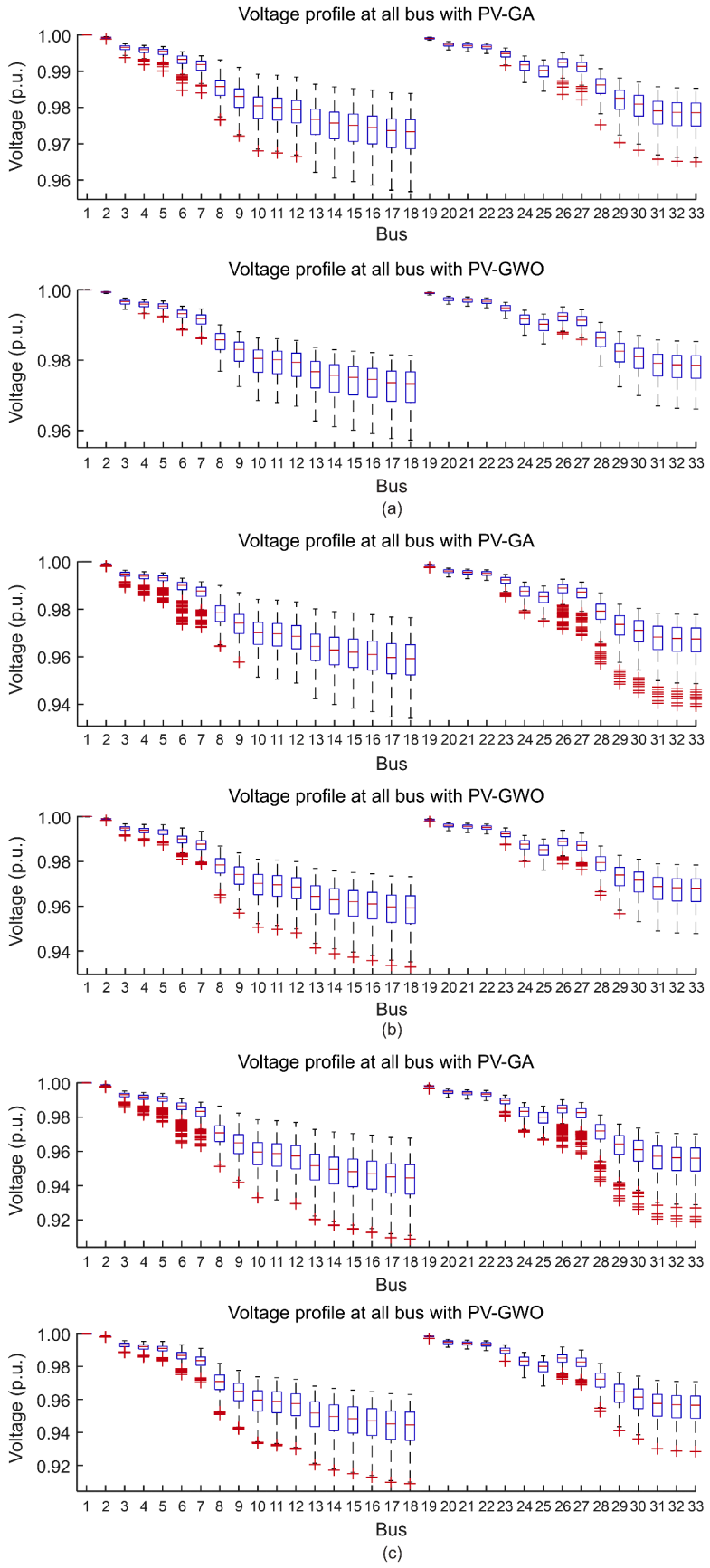

Fig. 18. Boxplots of fuzzy backward/forward sweep-genetic algorithm (F-BFS-GWO) and fuzzy backward/forward sweep-genetic algorithm (F-BFS-GA) for voltage profiles considering fuzzy load uncertainty. (a) Low, (b) medium, (c) high.

BFS-GWO and F-BFS-GA for residential load uncertainty in the 33-bus radial distribution network. Additionally, Figs. 16–18 illustrate the comparative performance of F-BFS-GWO and F-BFS-GA in terms of P_{loss}, Q_{loss}, and voltage profile possibilities under fuzzy load uncertainty scenarios at low, medium, and high loads. The benchmarking results between F-BFS-GWO and F-BFS-GA focused on the residential urban load sector under fuzzy load uncertainty.

The results in Table 6 demonstrate that F-BFS-GWO consistently yielded results similar to F-BFS-GA across all evaluated metrics.

Although the overall performance of F-BFS-GWO and GA appeared similar, F-BFS-GWO demonstrated notable advantages in terms of active power loss (P_{loss}), reactive power loss (Q_{loss}), and critical voltage regulation across all fuzzy load scenarios (low, medium, high). For example, F-BFS-GWO yielded slightly lower *P*max values under Medium and High load conditions, with *P*max reduced to 144.042 kW and 266.098 kW, respectively, compared to 144.595 kW and 268.309 kW obtained by GA. In terms of Q_{loss}, *Q*min and *Q*hp remained identical for both methods, but F-BFS–GWO produced slightly lower Qmax values under Medium and High load conditions. For example, in the medium-load case, Qhp was recorded at 39.943 kVar with GWO, compared to 40.876 kVar with GA, whereas in the high-load case, Qmax was recorded at 195.551 kVar with GWO, compared to 196.04 kVar. Regarding the voltage profiles, both optimizers resulted in comparable performance across all fuzzy scenarios. However, F-BFS-GWO maintained a slightly tighter voltage range under high load conditions, contributing to improved voltage regulation and enhanced system stability.

Sensitivity analysis helped to identify the optimal parameter ranges that maintained the solution quality under fuzzy uncertainty and confirmed the robustness of the GWO in practical applications. To further validate the robustness of the proposed F-BFS-GWO method, boxplots comparing the performance of F-BFS-GWO and F-BFS-GA in terms of P_{loss}, Q_{loss}, and voltage profiles under fuzzy load uncertainty at low, medium, and high loads were developed to visualize the effects of parameter variations on the output. In terms of robustness in uncertainty modeling, the GWO embedded within the fuzzy framework demonstrated greater flexibility and robustness across fuzzy load scenarios owing to its dynamic search behavior. This is evident in Figs. 16–18, which focus on the residential urban load for the benchmarking analysis.

Figs. 16 and 17 show the boxplots for the comparison of F-BFS-GA and F-BFS-GWO for the results of active and reactive power loss possibility considering fuzzy L, M, and H load uncertainties. In the comparative analysis between the methods, notable outliers were observed in the fuzzy active and reactive power loss results, particularly under high (H) and medium (M) load scenarios. These outliers represent suboptimal candidate solutions that are generated during the search process. In the active power loss (P_{loss}) and reactive power loss (Q_{loss}) graphs, F-BFS-GA exhibited wider variance and more pronounced outliers, especially in medium and high fuzzy load conditions. For example, under fuzzy L, M, and H load conditions, the GA produced 51, 84, and 131 outliers, respectively, with P_{loss} values that deviated significantly from the central cluster, indicating a tendency toward premature convergence or entrapment in local optima. In contrast, F-BFS-GWO demonstrated tighter clustering around the optimal region, with 13, 74, and 124 outliers for the L, M, and H load conditions, respectively, highlighting its consistency in navigating fuzzified solution spaces.

A similar trend was observed for reactive power loss. GA produced 51, 82, and 130 outliers under the L, M, and H load scenarios, respectively, whereas GWO resulted in 13, 76, and 121 fewer outliers, indicating more stable convergence and improved robustness in reactive power optimization under uncertainty.

In terms of critical voltage profile comparison, as depicted in Fig. 18, the outliers in the GA-based results occurred at weaker buses, particularly under high load conditions, where some voltage values dropped near or below 0.90 p.u., thus violating IEC recommended limits. In contrast, GWO produced voltage profiles with smoother transitions and fewer deviations, even under peak-load fuzziness, resulting in significantly fewer outlier data points.

Overall, the presence of more frequent outliers in the F-BFS-GA results suggested lower robustness to randomness and greater sensitivity to parameter tuning. In contrast, F-BFS-GWO demonstrated improved flexibility, greater robustness under uncertainty, and more consistent convergence behavior across all scenarios. These findings further justify the selection of GWO for optimal PVDG planning in fuzzy load environments. GWO demonstrated faster convergence, fewer outliers, and more consistent optimization performance across all fuzzy load scenarios. It maintained tighter voltage regulation and yielded slightly lower active and reactive power losses under medium- and high-load conditions. These strengths make the GWO more robust, efficient, and suitable for optimal PVDG allocation in uncertain distribution networks. The advantages observed make GWO a more suitable optimization method for fuzzy power flow applications in uncertain, multi-scenario distribution networks.

Although GWO demonstrated strong performance in simulation, its implementation in real distribution networks offers promising opportunities for further development and integration. The effectiveness of GWO can be enhanced by using real-time data from advanced metering infrastructure, supporting dynamic load and photovoltaic generation monitoring in operational settings. Its computational efficiency makes it suitable for near real-time applications, particularly when supported by high-performance computing infrastructure. Furthermore, integrating GWO into existing energy management systems can be facilitated through software interfacing that complies with regulatory standards and safety requirements for grid modernization initiatives.

4. Conclusion

A new hybrid F-BFS framework incorporating the GWO was developed for optimal PVDG allocation in a radial distribution system. The proposed method was validated on a 33-bus radial distribution network using real urban load profiles for residential, commercial, and industrial sectors in Malaysia. By modeling load uncertainties with triangular fuzzy membership functions, the approach effectively handled the uncertainties in both loads and PV generation. Uncertainty modeling successfully captured the typical consumption patterns of different load sectors based on usage behaviors. GWO was employed to optimize the placement and sizing of the PVDG units, minimize power losses, and improve voltage profiles. Under high (H) load conditions, the method achieved a total active power loss reduction of approximately 28.04% for residential, 46.06% for commercial, and 46.24% for industrial sectors with the highest membership degree in the fuzzy set. The voltage regulation also improved significantly approaching 1.0 p.u., particularly at critical buses. The membership function analysis further revealed that the range of power losses and critical voltage magnitudes varies across different load types, with residential areas suffering higher losses and voltage drops, followed by commercial and industrial loads, especially during high-demand periods. The novelty lies in combining fuzzified sector-based load modeling with a metaheuristic optimizer, which offers enhanced robustness compared to conventional deterministic or probabilistic methods. These results highlight the practical potential of this method for utilities aiming to improve distribution system efficiency under uncertainty. In the future, this framework can be extended to more complex networks, with further consideration of system failures, operational variations, and equipment-level uncertainties within the optimization process.

CRediT authorship contribution statement

Norhafidzah Mohd Saad: Writing – review & editing, Validation, Methodology, Formal analysis, Conceptualization, Visualization, Software, Investigation, Writing – original draft, Data curation. **Muhammad Alif Mat Yusuf:** Software, Visualization, Data curation, Writing – original draft, Validation, Formal analysis. **Mohammad Fadhil Abas:**

Validation, Data curation, Investigation, Conceptualization, Visualization, Software, Supervision, Methodology. **Dwi Pebrianti:** Supervision, Writing – review & editing, Conceptualization. **Norazila Jaalam:** Writing – original draft, Conceptualization, Writing – review & editing, Investigation. **Suliana Ab. Ghani:** Writing – original draft, Conceptualization, Writing – review & editing, Investigation.

Declaration of competing interest

The authors declare that they have no known competing financial interests or personal relationships that could have appeared to influence the work reported in this paper.

Acknowledgments

The authors express their gratitude to Universiti Malaysia Pahang Al-Sultan Abdullah and International Islamic University Malaysia for providing the research grant RDU223219.

References

[1] G. Allan, I. Eromenko, M. Gilmartin, et al., The economics of distributed energy generation: a literature review, Renew. Sustain. Energy Rev. 42 (2015) 543–556.
[2] N.O. Adelakun, B.A. Olanipekun, A review of solar energy, J. Multidiscip. Eng. Sci. Technol. 6 (2020) 11344–11347.
[3] I. Khenissi, T. Guesmi, I. Marouani, et al., Energy management strategy for optimal sizing and siting of PVDG-BES systems under fixed and intermittent load consumption profile, Sustainability 15 (2023) 1004.
[4] Z.X. Wang, W.R. Fan, Economic and environmental impacts of photovoltaic power with the declining subsidy rate in China, Environ. Impact Assess. Rev. 87 (2021) 106535.
[5] M. Fadaeenejad, M.A.M. Radzi, M.Z.A. AbKadir, et al., Assessment of hybrid renewable power sources for rural electrification in Malaysia, Renew. Sustain. Energy Rev. 30 (2014) 299–305.
[6] A.J. Abd Aziz, N.A. Baharuddin, R.M. Khalid, et al., Review of the policies and development programs for renewable energy in Malaysia: progress, achievements and challenges, Energy Explor. Exploit. 42 (2024) 1472–1501.
[7] I. Ortega-Romero, X. Serrano-Guerrero, A. Barragán-Escandón, et al., Optimal integration of distributed generation in long medium-voltage electrical networks, Energy Rep. 10 (2023) 2865–2879.
[8] Q. Nizamani, A.A. Hashmani, Z.H. Leghari, et al., Nature-inspired swarm intelligence algorithms for optimal distributed generation allocation: a comprehensive review for minimizing power losses in distribution networks, Alex. Eng. J. 105 (2024) 692–723.
[9] N.M. Saad, M.Z. Sujod, L. Ming, et al., Impacts of photovoltaic distributed generation location and size on distribution power system network, Int. J. Power Electron. Drive Syst. 9 (2018) 905.
[10] N.M. Saad, M.Z. Sujod, M.I.M. Ridzuan, et al., Optimization for distributed generation planning in radial distribution network using MVMO-SH, in: Proceedings of the IEEE 10th Control and System Graduate Research Colloquium (ICSGRC), Shah Alam, Malaysia, 2019, pp. 115–120.
[11] S. Kawambwa, R. Mwifunyi, D. Mnyanghwalo, et al., An improved backward/forward sweep power flow method based on network tree depth for radial distribution systems, J. Electr. Syst. Inf. Technol. 8 (2021) 7.
[12] S.M.F.S. Drus, N.M. Saad, M.F. Abas, et al., Distribution feeder reconfiguration with distributed generation using backward/forward sweep power flow–grey wolf optimizer, in: Proceedings of the 19th IEEE International Colloquium On Signal Processing & its Applications (CSPA), Kedah, Malaysia, 2023, pp. 213–218.
[13] C.M.A. Safwan, N.M. Saad, M. Abas, et al., Optimization of distributed generation using mix-integer optimization by genetic algorithm (MIOGA) considering load growth. Lecture Notes in Electrical Engineering B Series (LNEE), Springer Nature, Singapore, 2022, pp. 245–255.
[14] M. Al Amin Abdullah, N.M. Saad, M.F. Abas, et al., in: Optimization of radial distribution network with distributed generation using particle swarm optimization considering load growth, Springer, Singapore, 2022, pp. 57–268.
[15] Z. Mustaffa, M. Herwan, J. Isuwa, State of charge estimation of lithium-ion batteries in an electric vehicle using hybrid metaheuristic - deep neural networks models, Energy Storage Sav 4 (2025) 111–122.
[16] B.Z. Jin, X.J. Xu, Price forecasting through neural networks for crude oil, heating oil, and natural gas, Meas. Energy 1 (2024) 100001.
[17] B.Z. Jin, X.J. Xu, Forecasting wholesale prices of yellow corn through the Gaussian process regression, Neural Comput. Appl. 36 (2024) 8693–8710.
[18] A. Javaid, I. Shafi, I.U. Khalil, et al., Enhancing photovoltaic systems using Gaussian process regression for parameter identification and fault detection, Energy Reports 11 (2024) 4485–4499.
[19] N.M. Saad, M.Z. Sujod, M.I.M. Ridzuan, et al., Solar irradiance uncertainty management based on Monte Carlo-beta probability density function: case in Malaysian tropical climate, Bull. Electr. Eng. Inform. 8 (2019) 1135–1143.
[20] P. Maurya, P. Tiwari, A. Pratap, Electric eel foraging optimization algorithm for distribution network reconfiguration with distributed generation for power system performance enhancement considerations different load models, Comput. Electr. Eng. 119 (2024) 109531.
[21] A.F.A. Kadir, M. Fani, N. Ropidah, et al., Analysis of load variation consideration for optimal distributed generation placement, Int. J. Adv. Comput. Sci. Appl. 12 (2021) 366–372.
[22] J.Q. Fu, Y. Han, W.H. Li, et al., A novel optimization strategy for line loss reduction in distribution networks with large penetration of distributed generation, Int. J. Electr. Power Energy Syst. 150 (2023) 109112.
[23] N. Jaalam, A.Z. Ahmad, A.M.A. Khalid, et al., Low voltage ride through enhancement using grey wolf optimizer to reduce overshoot current in the grid-connected PV system, Math. Probl. Eng. 2022 (2022) 3917775.
[24] A. Chibani, S. Merouani, H. Laidoudi, et al., Analysis and optimization of concentrator photovoltaic system using a phase change material (RT 35HC) combined with variable metal fins, J. Energy Storage 72 (2023) 108283.
[25] B.W. Tuinema, J.L. Rueda Torres, A.I. Stefanov, et al.. Probabilistic Reliability Analysis of Power Systems, Springer, Berlin, 2020.
[26] N.M. Saad, M.Z. Sujod, M.I. Muhammad Ridzuan, et al., A new optimisation framework based on Monte Carlo embedded hybrid variant mean–variance mapping considering uncertainties, Decis. Anal. J. 10 (2024) 100368.
[27] M.I. Muhammad Ridzuan, N.N.R. Roslan, N.F. Mohd Fauzi, et al., Reliability-based DG location using Monte-Carlo simulation technique, SN Appl. Sci. 2 (2020) 145.
[28] M.I. Muhammad Ridzuan, M.A.Z. Rusli, N.M. Saad, Reliability performance of low voltage (LV) network configuration, in: Proceedings of the ECCE2019, Lecture Notes in Electrical Engineering, Springer, Singapore, 2020, pp. 83–793.
[29] H. Yin, Y. Wang, G. Wu, et al., Distributed optimal operation of PV-storage-load micro-grid considering renewable and load uncertainties, J. Energy Storage 86 (2024) 111168.
[30] H. Li, Z. Zhang, X.G. Yin, A novel probabilistic power flow algorithm based on principal component analysis and high-dimensional model representation techniques, Energies 13 (2020) 3520.
[31] T. Badings, T.D. Simão, M. Suilen, et al., Decision-making under uncertainty: beyond probabilities, Int. J. Softw. Tools Technol. Transf. 25 (2023) 375–391.
[32] H.Y. Wu, P. Dong, M.B. Liu, Random fuzzy power flow of distribution network with uncertain wind turbine, PV generation, and load based on random fuzzy theory, IET Renew. Power Gener. 12 (2018) 1180–1188.
[33] M.I. Zaki, R.A. El Sehiemy, T.F. Megahed, et al., A proposed fault identification-based fuzzy approach for active distribution networks with photovoltaic systems, Measurement 223 (2023) 113678.
[34] M. Sedaghat, E. Rokrok, M. Bakhshipour, A new DG allocation approach based on biogeography-based optimization with considering fuzzy load uncertainty, IAES Int. J. Artif. Intell. 4 (2015) 89.
[35] R.K. Samala, M.R. Kotapuri, Optimal allocation of distributed generations using hybrid technique with fuzzy logic controller radial distribution system, SN Appl. Sci. 2 (2020) 191.
[36] M. Alkayyali, T.A. Tutunji, PSO-based algorithm for inverse kinematics solution of robotic arm manipulators, in: Proceedings of the 20th International Conference on Research and Education in Mechatronics (REM), Wels, Austria, IEEE, 2019, pp. 1–6.
[37] M. Maher, M.A. Ebrahim, E.A. Mohamed, et al., Ant-lion optimizer based optimal allocation of distributed generators in radial distribution networks, Int. J. Eng. Inf. Syst. 1 (2017) 225–238.
[38] D. Shirmohammadi, H.W. Hong, A. Semlyen, et al., A compensation-based power flow method for weakly meshed distribution and transmission networks, IEEE Trans. Power Syst. 3 (1988) 753–762.
[39] S. Mirjalili, S.M. Mirjalili, A. Lewis, Grey wolf optimizer, Adv. Eng. Softw. 69 (2014) 46–61.
[40] M.E. Baran, F.F. Wu, Network reconfiguration in distribution systems for loss reduction and load balancing, IEEE Trans. Power Deliv. 4 (1989) 1401–1407.